

Chalcogen Bonding in Co-Crystals: Activation through 1,4-Perfluorophenylene vs. 4,4 '-Perfluorobiphenylene Cores

Arun Dhaka, Olivier Jeannin, Emmanuel Aubert, Enrique Espinosa, Marc Fourmigue

▶ **To cite this version:**

Arun Dhaka, Olivier Jeannin, Emmanuel Aubert, Enrique Espinosa, Marc Fourmigue. Chalcogen Bonding in Co-Crystals: Activation through 1,4-Perfluorophenylene vs. 4,4 '-Perfluorobiphenylene Cores. Molecules, 2021, 26 (13), pp.4050. 10.3390/molecules26134050 . hal-03330992

HAL Id: hal-03330992
https://hal.science/hal-03330992

Submitted on 1 Sep 2021

HAL is a multi-disciplinary open access archive for the deposit and dissemination of scientific research documents, whether they are published or not. The documents may come from teaching and research institutions in France or abroad, or from public or private research centers.

L'archive ouverte pluridisciplinaire **HAL**, est destinée au dépôt et à la diffusion de documents scientifiques de niveau recherche, publiés ou non, émanant des établissements d'enseignement et de recherche français ou étrangers, des laboratoires publics ou privés.



Distributed under a Creative Commons Attribution 4.0 International License

molecules

MDPI

Article

Chalcogen Bonding in Co-Crystals: Activation through 1,4-Perfluorophenylene vs. 4,4′-Perfluorobiphenylene Cores

Arun Dhaka [1], Olivier Jeannin [1], Emmanuel Aubert [2], Enrique Espinosa [2] and Marc Fourmigué [1,*]

[1] CNRS, ISCR (Institut des Sciences Chimiques de Rennes) UMR 6226, Univ Rennes, 35000 Rennes, France; arun.dhaka@univ-rennes1.fr (A.D.); olivier.jeannin@univ-rennes1.fr (O.J.)
[2] CNRS, CRM2, Université de Lorraine, 54000 Nancy, France; emmanuel.aubert@univ-lorraine.fr (E.A.); enrique.espinosa@univ-lorraine.fr (E.E.)
* Correspondence: marc.fourmigue@univ-rennes1.fr

Abstract: The ability of alkylseleno/alkyltelluroacetylenes such as bis(selenomethylethynyl)-perfluorobenzene (**4F-Se**) to act as a ditopic chalcogen bond (ChB) donor in co-crystals with ditopic Lewis bases such as 4,4′-bipyridine is extended here to the octafluorobiphenylene analog, 4,4′-bis(selenomethylethynyl)-perfluorobiphenyl (**8F-Se**), with the more electron-rich 4,4′-bipyridylethane (**bpe**), showing in the 1:1 (**8F-Se**)•(**bpe**) co-crystal a shorter and more linear C−Se•••N ChB interaction than in (**4F-Se**)•(**bpe**), with Se•••N distances down to 2.958(2) Å at 150 K, i.e., a reduction ratio of 0.85 vs. the van der Waals contact distance.

Keywords: chalcogen bonding; sigma-hole activation; crystal engineering; Lewis-base

check for updates

Citation: Dhaka, A.; Jeannin, O.; Aubert, E.; Espinosa, E.; Fourmigué, M. Chalcogen Bonding in Co-Crystals: Activation through 1,4-Perfluorophenylene vs. 4,4′-Perfluorobiphenylene Cores. *Molecules* **2021**, *26*, 4050. https://doi.org/10.3390/molecules26134050

Academic Editors: Ryan Groeneman and Eric Reinheimer

Received: 16 June 2021
Accepted: 30 June 2021
Published: 2 July 2021

Publisher's Note: MDPI stays neutral with regard to jurisdictional claims in published maps and institutional affiliations.

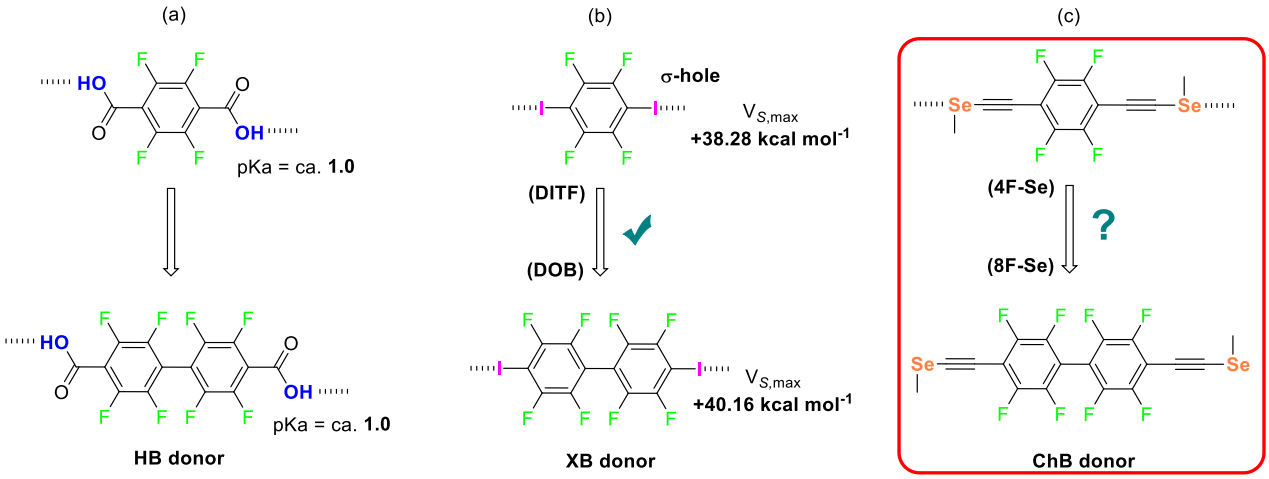
Copyright: © 2021 by the authors. Licensee MDPI, Basel, Switzerland. This article is an open access article distributed under the terms and conditions of the Creative Commons Attribution (CC BY) license (https://creativecommons.org/licenses/by/4.0/).

1. Introduction

Crystal engineering strategies are manifested by the choice of intermolecular interactions owing to their strength, directionality and predictability that allow one to transfer the packing instructions in a molecule [1]. In this context, halogen bond (XB) [2,3], a subset of sigma-hole interactions, has emerged as an indispensable tool due to its significant linear directionality and tuneable sigma-hole activation that opens the door for a wide range of applications [4–6]. Similarly, chalcogen bond (ChB) [7] is an interaction between an electron-depleted site of an activated chalcogen atom and an electron-rich site of a Lewis-base [8,9]. Chalcogen bond, being a sister non-covalent interaction to halogen bond [10,11], has been mostly targeted to follow the trails of halogen bond in the field of crystal engineering but it is often limited by the presence of two sigma holes on chalcogen atoms. At variance with mono-valent halogen atoms, one extra valency of Se/Te can indeed invite additional changes in crystal packing that consequently dilutes the predictability of ChB interaction. Furthermore, organic selenides/tellurides are more reactive and are synthetically far less investigated compared to organic halides. Despite that, over the years, interesting ChB donors have been developed and some earlier examples include $S(CN)_2$ [12], $Se(CN)_2$ [13], 1,2,5-chalcogenadiazoles [14,15], 1,2-chalcogenazole N-oxides [16,17], or alkyltelluroalkynyl derivatives [18,19] that self-associate into discrete solid-state structures. To recover the linear directionality characteristic of halogen bonding interactions, chalcogen atoms are typically disymmetrized with only one strongly electron-withdrawing substituent to force a digger electron depletion along one favored single direction, as recently observed in organic selenocyanates, such as 1,4-*bis*(selenocyanatomethyl)-benzene that forms 1-D chains with 4,4′-bipyridine through short and directional Se•••N contacts [20–23]. The interaction strength parallels the degree of activation in both donor and acceptor molecules, an aspect often used in crystal engineering to quantify the robustness of a supramolecular motif.

In this regard, hydrogen and halogen bonding interactions have been extensively utilized to selectively tune the strength of intermolecular interactions in co-crystals by systematically treating either a donor with various acceptors of different Lewis-base character

or an acceptor with various donors exhibiting different modes of activation. However, chalcogen bonding still remains less explored in this direction and one such example includes a recent study by Bryce et al. on investigations of ChB strength in a series of co-crystals between 3,4-dicyano-1,2,5-seleno/telluro-diazole acting as ChB donor and various N-oxide and pyridyl derivatives acting as ChB acceptors [24,25]. Rigid ChB donors such as alkylseleno/alkyltelluroacetylenes were recently demonstrated to exhibit a strong-sigma hole activation and remarkable control of directionality in co-crystal formation with bipyridyl derivatives, allowing for a fine tuning of Ch•••N interaction strength within the chalcogen-bonded 1-D chain motif [26]. In addition, a recent investigation of the U-shaped ChB donor 1,8-bis(telluromethylethynyl)-anthracene (BTMEA) with a series of (strong to weak) bipyridyl derivatives suggested that the strongest Te•••N interaction was indeed associated with the strongest Lewis-base used in this study [27]. Such fundamental studies become very crucial to understanding the limitations of chalcogen bond formed under different chemical and electronic environments. Surprisingly, the reverse situation where ChB strength can be tuned in a supramolecular motif through structural modification of the chalcogen bond donor itself is much less explored. In this context, an interesting example based on XB (Scheme 1b) showed that sigma-hole on iodine atom is rather enhanced when moving from 1,4-diiodotetrafluorobenzene (**DITF**) to 4,4′-diiodooctafluorobiphenyl (**DOB**) that incorporates a stronger activating core. This was also evident from $V_{S,max}$ values of +38.28 and +40.16 kcal mol^{-1} (mapped on the electron density surface cut at the 0.002 e/Å^3 level) observed for **DITF** and **DOB** respectively [28]. Additionally, their co-crystals with nicotine (**A1**), formed through halogen bonds, reveal that the strongest N•••I interaction was present in the structure of **DOB**•A1 with distance 2.808 Å (RR = 0.79) vs. 2.869 Å (RR = 0.81) found in **DITF**•A1 [28]. On contrary, a study by Aakeroy et al. on a series of co-crystals between these XB donors and heteroaryl-2-imidazoles (**A2**), driven through XB and HB, revealed that the strongest N•••I interaction was always associated with **DITF**•A2 structures in contrast to **DOB**•A2 co-crystals [29]. Hence, although the electrostatic surface potential suggests a stronger sigma-hole activation in **DOB** over **DITF**, this information is not explicitly reflected in their ability to form co-crystals with Lewis-base. Another element of comparison is brought by the pKa_1 values of their analogous dicarboxylic acid derivatives (Scheme 1a) which were estimated to be approximately the same, indicating a negligible effect of the core on hydrogen bonding behavior [30].



Scheme 1. Activation through 1,4-perfluorophenylene vs. 4,4′-octaperfluorobiphenylene in different types of intermolecular interactions: (**a**) hydrogen bonding, (**b**) halogen bonding and (**c**) chalcogen bonding. See reference [28] for calculated $V_{S,max}$ values for **DITF** and **DOB**.

Inspired by these results, we present herein a case study on the modulation of chalcogen bond with respect to the activation core in two ChB donors, namely 1,4-bis(selenomethy

lethynyl)-perfluorobenzene (**4F-Se**) vs. 4,4′-bis(selenomethylethynyl)-perfluorobiphenyl (**8F-Se**) (Scheme 1c).

2. Results and Discussions

The tendency of a molecule to engage in different types of intermolecular non-covalent interactions where electrostatics, besides dispersion, play a significant role can primarily be anticipated by mapping the electrostatic potential (ESP) on molecular surfaces. ESP calculations for our two ChB donors revealed the presence of a significant σ-hole on the Se atoms along the (C≡C)−Se bond with $V_{S,max}$ values of +35.7 kcal mol^{-1} and +37.4 kcal mol^{-1} for donors **4F-Se** and **8F-Se** respectively (Figure 1). These values clearly indicate a comparatively larger activation of the σ-hole in **8F-Se**, demonstrating that the perfluorobiphenyl core plays an additional activating effect with respect to the perfluorophenyl one incorporated in **4F-Se.** A less significant second σ-hole is also present along the CH_3−Se bonds in both **4F-Se** and **8F-Se** donors, with $V_{S,max}$ values of respectively +18.45 kcal mol^{-1} and +20.2 kcal mol^{-1} establishing potentially a secondary directional preference of these donors toward molecular assembly.

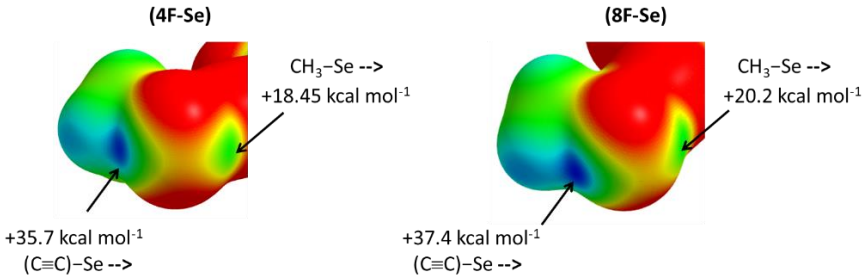
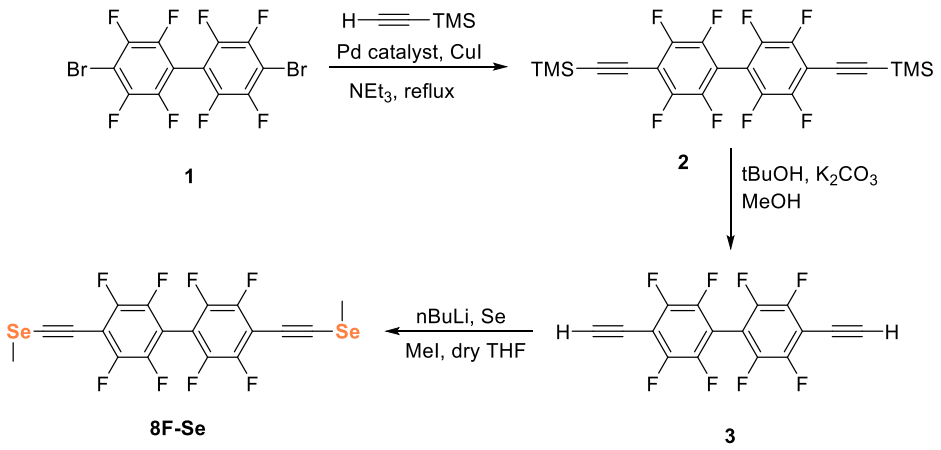


Figure 1. Electrostatic potential map of **BTMEA** in an optimized geometry showing the deep electron-depleted area (blue regions) in the prolongation of (C≡C)−Se bonds and a less significant one in the prolongation of the (CH_3)−Se bonds. Color range from 0.0 (red) to 37.7kcal/mol (blue) and isosurfaces of electron density at ϱ = 0.002 a.u.

The synthesis of the new ChB donor **8F-Se** is outlined in Scheme 2 and starts with commercially available 4,4′-dibromoperfluorobiphenyle to first obtain compound **2** through Sonogashira coupling reaction. Subsequently, silyl deprotection followed by lithiation with Se metal and alkylation with MeI furnished the desired donor **8F-Se** in good yield. The same strategy starting with 1,4-diiodotetrafluorobenzene is then followed to obtain **4F-Se** as described in our previous report [26].



Scheme 2. Synthesis route to the ChB donor **8F-Se**.

Molecule **8F-Se** crystallizes in the triclinic system (SG $P\bar{1}$) into 1-D chains driven through Se●●●Se contacts with the shortest intermolecular distance at 3.429 Å, which

corresponds to a reduction ratio (RR) of 0.90 relative to the sum of van der Waals radii (2 × 1.90(Se) = 3.80 Å). The C−Se•••Se bond angle values of 164.3° and 158.1° suggest these Se•••Se interactions to be of type-I (Figure 2). The molecule is in general position with a torsion angle of 57.54° between both aromatic rings. Concerning the crystal structure of donor **4F-Se**, two different polymorphs in monoclinic (SG $P2_1/c$) and tetragonal (SG $I4_1/a$) systems were reported in our previous paper [26].

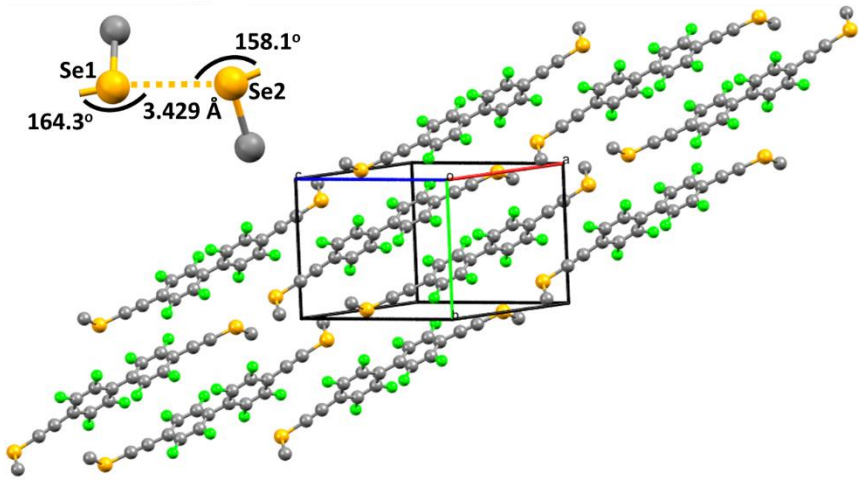


Figure 2. Crystal packing of **8F-Se** showing type-I Se•••Se interactions. Hydrogens are omitted for clarity.

To further evaluate this difference in sigma-hole activation, we decided to co-crystallize both donors with various ditopic Lewis-bases to assess their ability to form chalcogen bonded 1D chains. We could obtain co-crystals from both ChB donors **4F-Se** and **8F-Se** with the 1,2-bis(4-pyridyl)ethane (**bpe**) as Lewis-base. Data were collected for both co-crystals at room temperature and at 150 K, in order to evaluate also the evolution of the ChB interaction with temperature.

4F-Se•bpe crystallizes in the monoclinic system, SG $P2_1/n$, with both molecules located on inversion centers, while **8F-Se•bpe** crystallizes in the monoclinic system, SG C2/c, with the **bpe** molecule located on an inversion center and the **8F-Se** Ch donor on a 2-fold axis. The torsion angle between the two aromatic rings in **8F-Se** amounts to 57.5(1)° at RT and to 55.4(1)° at 150 K, i.e., very close to that found in the crystal structure of **8F-Se**. Both co-crystallizations with **bpe** resulted in the formation of 1:1 cocrystals **4F-Se•bpe** and **8F-Se•bpe**. In both systems, the 1D chains assembled by ChB motifs develop through short Se•••N contacts (Table 1) with intermolecular distances at RT of 3.052(2) Å in **4F-Se•bpe** and a shorter 3.029(4) Å distance in case of **8F-Se•bpe,** suggesting a stronger activation of the σ-hole in Se-atoms in the latter (Figure 3). This slight strengthening with the **8F-Se** ChB donor is enhanced at low temperatures (150 K) with the Se•••N distances decreasing to 3.005(2) and 2.958(2) Å in **4F-Se•bpe** and **8F-Se•bpe**, respectively.

Table 1. Structural characteristics of the ChB interactions in co-crystals.

Co-Crystal	T (K)	Se•••N dist. (Å)	RR	C−(Se)•••N Angle (°)
4F-Se•bpe	296	3.052 (2)	0.88	172.1 (1)
8F-Se•bpe	296	3.029 (4)	0.87	176.7 (1)
4**F-Se•**bpe	150	3.005 (2)	0.87	172.7 (1)
8F-Se•bpe	150	2.958 (2)	0.85	177.3 (1)

The strength of the Se•••N interactions in these 1D motifs is also manifested by their almost linear directionality, as the (C≡)C−Se•••N angles are very close to 180° with **4F-Se**, and even closer with **8F-Se** (Table 1).

In conclusion, it appears that replacement of the p-tetrafluorophenylene core in **4F-Se** by the extended p-octafluorobiphenylene one in **8F-Se** not only preserves the robustness of the 1D chalcogen-bonded motif in cocrystals with ditopic Lewis bases such as bpe, but also strengthens it, albeit to a limited extend. This strengthening provides, however, an incentive to prepare even longer ChB donors based on these (chalcogenoalkyl)alkynyl derivatives, toward the elaboration of more complex, eventually porous, systems stabilized by such non-bonding σ-hole-based intermolecular interactions.

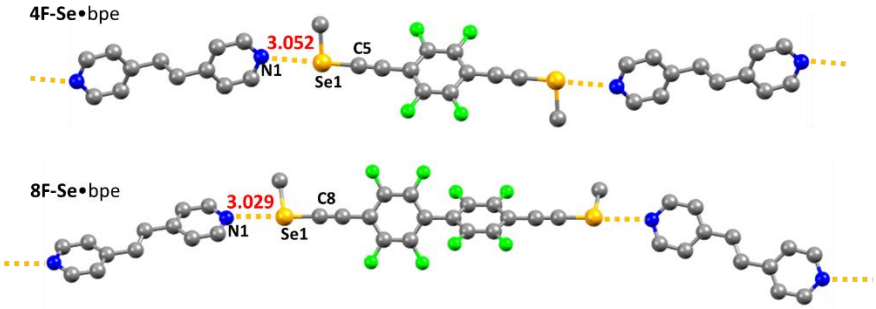


Figure 3. Details of the solid-state structures of 1:1 co-crystals of **bpe** with **4F-Se** and **8F-Se** at RT. Hydrogens atoms are omitted for clarity.

3. Materials and Methods

General Information. Oxygen- and moisture-sensitive experiments were carried out under a dry oxygen-free nitrogen atmosphere using standard Schlenk techniques. THF was dried using a commercial solvent purification system from Inert Technology. The NMR spectra were recorded on Bruker spectrometers (300 MHz, Bruker, Mannheim, Germany) referenced to residual solvent signals as internal standards. Elemental analyses were performed at BioCIS (Elementar Vario/Perkin Elmer 2400 series, PerkinElmer, Watham, MA, USA). Commercially available compounds 4,4′-dibromoperfluorobiphenyl, 1,2-bis(4-pyridyl)ethane (bpe) and anhydrous triethylamine were purchased and used as received.

4,4′-Bis(trimethylsilylethynyl)-perfluorobiphenylene **2**. 4,4′-dibromoperfluorobephenyl (1.5 g, 3.3 mmol) was placed in an oven-dried 100 mL round bottom flask. Anhydrous trimethylamine (50 mL) was added under argon followed by TMS-acetylene (1.4 mL, 9.86 mmol, 3 eq). $PdCl_2(PPh_3)$ (230 mg, 0.32 mmol, 0.1 eq.) and CuI (62 mg, 0.32 mmol, 0.1 eq.) were then added to the reaction mixture under argon and the mixture was refluxed overnight. The reaction mixture was cooled down to room temperature and the precipitate formed was filtered off. Trimethylamine was evaporated using rotary evaporator under reduced pressure and the crude solid residue was subjected to flash column chromatography on silica gel for purification (eluent: petroleum ether) to afford **2** (1.1 g, 70%) as a white solid. R_f = 0.5 (petroleum ether); ^{1}H NMR (300 MHz, $CDCl_3$): δ 0.33 (s, 18H); ^{19}F NMR (300 MHz, $CDCl_3$): δ −135.5, −138.5.

4,4′-Diethynylperfluorobiphenylene **3**. Compound **2** (150 mg, 0.30 mmol) was dissolved in tert-butanol (20 mL) under argon, and potassium carbonate (400 mg, 2.9 mol, 9.6 eq.) was added at 30°C. Reaction was monitored by TLC and 0.1 mL of MeOH was added in an interval of one hour until all the starting material was consumed. Caution: Use of methanol in excess results in the formation of the methoxyacetylene derivative. Reaction mixture was filtered over Celite® and the solution was evaporated using rotary evaporator under reduced pressure. The residue was subjected to flash column chromatography on silica gel (eluent: petroleum ether) for purification to afford **3** (94 mg, 89%) as white solid. R_f = 0.4 (petroleum ether); ^{1}H NMR (300 MHz, $CDCl_3$): δ 3.78 (s, 2H); ^{19}F NMR (300 MHz, $CDCl_3$): δ −135.1, −137.8.

4,4′-Bis(selenomethylethynyl)-perfluorobiphenylene **8F-Se**. Compound **3** (240 mg, 0.69 mmol) was placed in an oven-dried 100 mL round bottom flask under inert atmosphere. Dry THF (20 mL) was added under argon flow and the solution was cooled to −78 °C. A solution of nBuLi (2.5 M in hexane, 0.624 mL, 1.52 mmol, 2.2 eq.) was added and the reaction mixture was stirred for half an hour. A finely ground dry Se powder (120 mg, 1.52 mmol, 2.2 eq.) was added under argon flow at −78 °C and the reaction mixture was gradually allowed to warm to RT. After 5 h, MeI (0.094 mL, 1.52 mmol, 2.2 eq.) was added dropwise to the dark red solution and stirring was continued overnight. Reaction was quenched with saturated aqueous ammonium chloride solution (5 mL for 1 mmol of alkyne). The mixture was extracted with diethyl ether (2 × 30 mL). The combined organic layers were dried over Na_2SO_4, filtered and concentrated under reduced pressure. The obtained crude product was subjected to column chromatography (eluent: petroleum-ether) to afford **8F-Se** (120 mg, 52%) as light-yellow solid. R_f = 0.3 (petroleum ether). Mp: 142–144 °C; ^{1}H NMR (300 MHz, $CDCl_3$): δ 2.49 (s, 6H); ^{19}F NMR (300 MHz, $CDCl_3$): δ −136.6, −138.5. ^{13}C NMR (300 MHz, $CDCl_3$): δ 10.2, 83.2, 89.2, 106.9, 142.2, 145.4, 148.6. Anal. Calcd. for $C_{18}H_6F_8Se_2$: C, 40.62; H, 1.14; found: C, 41.73; H, 1.31. The slightly too large C content can be attributed to some partial decomposition.

4,4′-Bis(selenomethylethynyl)-perfluorobenzene **4F-Se**. This was synthesized following the same strategy starting with 1,4-diiododtetrafluorobenzene, as also described in the previous report [26].

Co-crystal Preparation

4F-Se•bpe. To a solution of **4F-Se** (7 mg) in EtOAc (0.5 mL) was layered with 1,2-bis(4-pyridyl)ethane (3.3 mg, 1 equiv.) dissolved in EtOAc (0.5 mL). Slow evaporation of solvent resulted in the formation of yellow plate-shaped crystals. Mp: 103 °C; Anal. Calcd. for $C_{24}H_{18}F_4N_2Se_2$: C, 50.72; H, 3.19; N, 4.93; found: C, 49.40; H, 3.49; N, 4.47.

8F-Se•bpe. To a solution of **8F-Se** (9 mg) in EtOAc (0.5 mL) was layered with 1,2-bis(4-pyridyl)ethane (3.1 mg, 1 equiv.) dissolved in EtOAc (0.5 mL). An overnight slow evaporation of solvent resulted in the formation of yellow plate-shaped crystals. Mp: 125–127 °C. Anal. Calcd. for $C_{30}H_{18}F_8N_2Se_2$: C, 50.29; H, 2.53; N, 3.91; found: C, 50.52; H, 2.62; N, 3.86.

Crystallography

Data collections at RT were performed on an APEXII Bruker-AXS diffractometer (Mannheim, Germany) equipped with a CCD camera and data collections at 150 K on a D8 VENTURE Bruker AXS diffractometer. Structures were solved by direct methods using the SIR97 program and then refined with full-matrix least-square methods based on F^2 (SHELXL-97) [31] with the aid of the WINGX program [32]. All non-H atoms of the molecules were refined anisotropically, and hydrogen atoms were introduced at calculated positions (riding model), included in the structure factor calculations but not refined. Details about data collection and solution refinement are given in Table 2. CCDC No. 2090416-2090420. contains the supplementary crystallographic data for this paper. These data can be obtained free of charge via http://www.ccdc.cam.ac.uk/conts/retrieving.html.

Theoretical Calculations

Molecular structures of **4F-Se** and **8F-Se** have been optimized in gas phase (vacuum) with Gaussian 09 software using density functional theory [33]. B3LYP functional was used, completed with D3 dispersion Grimme dispersion correction [34]. The def2-TZVPP basis set was employed for all atoms. Frequency calculations were performed in order to check that true energy minima were obtained. Isosurfaces of electron density (ϱ = 0.002 a.u.) mapped with the corresponding total electrostatic potential were calculated and drawn with AIMAll software [35].

Table 2. Summary of crystal data.

Title 1	8F-Se	4F-Se•bpe (RT)	4F-Se.bpe (150 K)	8F-Se•bpe (RT)	8F-Se•bpe (150 K)
CCDC number	2090416	2090417	2090418	2090419	2090420
Formula	$C_{18}H_6F_8Se_2$	$C_{24}H_{18}F_4N_2Se_2$	$C_{24}H_{18}F_4N_2Se_2$	$C_{30}H_{18}F_8N_2Se_2$	$C_{30}H_{18}F_8N_2Se_2$
FW	532.15	568.32	568.32	716.38	716.38
Crystal system	triclinic	monoclinic	monoclinic	monoclinic	monoclinic
Space group	$P\bar{1}$	$P2_1/n$	$P2_1/n$	$C2/c$	$C2/c$
a/Å	8.4551 (6)	12.6631 (8)	12.6624 (16)	22.529 (2)	21.575 (2)
b/Å	8.6842 (5)	5.7143 (4)	5.6541 (8)	6.2237 (6)	6.1938 (5)
c/Å	12.4001 (9)	16.6845 (13)	16.341 (2)	21.539 (3)	21.412 (2)
α/°	91.956 (2)	90.00	90.00	90.00	90.00
β /°	108.704 (2)	105.503 (4)	105.367 (4)	105.862 (7)	105.762 (3)
γ /°	94.837 (2)	90.00	90.00	90.00	90.00
V/Å^3	857.52 (10)	1163.38 (14)	1128.1 (3)	2905.1 (6)	2753.7 (4)
Z	2	2	2	4	4
D_c/g cm^{-3}	2.061	1.622	1.673	1.638	1.728
T/K	150 (2)	296 (2)	150 (2)	296 (2)	150 (2)
μ / mm^{-1}	4.395	3.224	3.325	2.620	2.764
F(000)	508	560	560	1408	1408
Refl. collected	40049	7490	7242	13879	18466
Refl. indep. (R_{int})	3944 (0.0583)	2635 (0.0489)	2570 (0.0409)	3295 (0.0439)	3152 (0.0426)
Refl. Obs. [I > 2σ(I)]	3449	1779	1985	2005	2568
GOF on F^2	1.076	1.018	1.046	1.014	1.126
R_1 [I > 2σ(I)] (all)	0.0264 (0.0332)	0.0453 (0.080)	0.0373 (0.0559)	0.0419 (0.0842)	0.0333 (0.0452)
wR_2 [I > 2σ(I)] (all)	0.0608 (0.0651)	0.0966 (0.107)	0.0795 (0.0853)	0.1031 (0.1224)	0.0680 (0.0725)
$\Delta\varrho_{max,min}$/e Å^{-3}	+0.508, −0.933	+0.899, −0.606	+0.561, −0.514	0.546, −0.297	+0.573, −0.461

Author Contributions: A.D. and M.F. conceived the project; A.D. designed and performed the syntheses and crystal growth experiments, he analyzed the solid-state organizations; O.J. carried out the crystallographic studies; E.A. and E.E. carried out and analyzed the ESP calculations; A.D. and M.F. wrote the manuscript, with contributions from all the authors. All authors have read and agreed to the published version of the manuscript.

Funding: This work has been supported by ANR (France) under contracts numbers ANR-17-CE07-0025-01 (Nancy) and ANR-17-CE07-0025-02 (Rennes). The EXPLOR mesocentre is thanked for computing facilities (Project 2019CPMXX0984).

Institutional Review Board Statement: Not applicable.

Informed Consent Statement: Not applicable.

Data Availability Statement: Data is contained within the article.

Acknowledgments: We thank the CDIFX (Rennes) for access to the single crystal X-ray diffraction facilities.

Conflicts of Interest: The authors declare no conflict of interest.

Sample Availability: Samples of the compounds are available from the authors upon request.

References

1. Desiraju, G.R. Crystal Engineering: From Molecule to Crystal. *J. Am. Chem. Soc.* **2013**, *135*, 9952–9967. [CrossRef] [PubMed]
2. Desiraju, G.R.; Ho, P.S.; Kloo, L.; Legon, A.C.; Marquardt, R.; Metrangolo, P.; Politzer, P.; Resnati, G.; Rissanen, K. Definition of the Halogen Bond (IUPAC Recommendations 2013). *Pure Appl. Chem.* **2013**, *85*, 1711–1713. [CrossRef]
3. Cavallo, G.; Metrangolo, P.; Milani, R.; Pilati, T.; Priimagi, A.; Resnati, G.; Terraneo, G. The Halogen Bond. *Chem. Rev.* **2016**, *116*, 2478–2601. [CrossRef]
4. Gilday, L.C.; Robinson, S.W.; Barendt, T.A.; Langton, M.J.; Mullaney, B.R.; Beer, P.D. Halogen Bonding in Supramolecular Chemistry. *Chem. Rev.* **2015**, *115*, 7118–7195. [CrossRef]
5. Priimagi, A.; Cavallo, G.; Metrangolo, P.; Resnati, G. The Halogen Bond in the Design of Functional Supramolecular Materials: Recent Advances. *Acc. Chem. Res.* **2013**, *46*, 2686–2695. [CrossRef]
6. Fourmigué, M. Halogen Bonding: Recent Advances. *Curr. Op. Solid State Mater. Sc.* **2009**, *13*, 36–45. [CrossRef]
7. Aakeroy, C.B.; Bryce, D.L.; Desiraju, G.R.; Frontera, A.; Legon, A.C.; Nicotra, F.; Rissanen, K.; Scheiner, S.; Terraneo, G.; Metrangolo, P.; et al. Definition of the Chalcogen Bond (IUPAC Recommendations 2019). *Pure Appl. Chem.* **2019**, *91*, 1889–1892. [CrossRef]

8. Vogel, L.; Wonner, P.; Huber, S.M. Chalcogen Bonding: An Overview. *Angew. Chem. Int. Ed.* **2019**, *58*, 1880–1891. [CrossRef]
9. Fourmigué, M.; Dhaka, A. Chalcogen Bonding in Crystalline Diselenides and Selenocyanates: From Molecules of Pharmaceutical Interest to Conducting Materials. *Coord. Chem. Rev.* **2020**, *403*, 213084. [CrossRef]
10. Wang, W.; Ji, B.; Zhang, Y. Chalcogen Bond: A Sister Noncovalent Bond to Halogen Bond. *J. Phys. Chem. A* **2009**, *113*, 8132–8135. [CrossRef]
11. Scilabra, P.; Terraneo, G.; Resnati, G. The Chalcogen Bond in Crystalline Solids: A World Parallel to Halogen Bond. *Acc. Chem. Res.* **2019**, *52*, 1313–1324. [CrossRef] [PubMed]
12. Alikhani, E.; Fuster, F.; Madebene, B.; Grabowski, S.J. Topological Reaction Sites–Very Strong Chalcogen Bonds. *Phys. Chem. Chem. Phys.* **2014**, *16*, 2430–2442. [CrossRef] [PubMed]
13. Burchell, C.J.; Kilian, P.; Slawin, A.M.Z.; Woollins, J.D.; Tersago, K.; Van Alsenoy, C.; Blockhuys, F. E2(CN)2 (E = S, Se) and Related Compounds. *Inorg. Chem.* **2006**, *45*, 710–716. [CrossRef] [PubMed]
14. Cozzolino, A.F.; Vargas-Baca, I.; Mansour, S.; Mahmoudkhani, A.H. The Nature of the Supramolecular Association of 1,2,5-Chalcogenadiazoles. *J. Am. Chem. Soc.* **2005**, *127*, 3184–3190. [CrossRef] [PubMed]
15. Garrett, G.E.; Gibson, G.L.; Straus, R.N.; Seferos, D.S.; Taylor, M.S. Chalcogen Bonding in Solution: Interactions of Benzotelluradiazoles with Anionic and Uncharged Lewis Bases. *J. Am. Chem. Soc.* **2015**, *137*, 4126–4133. [CrossRef]
16. Ho, P.C.; Szydlowski, P.; Sinclair, J.; Elder, P.J.W.; Kübel, J.; Gendy, C.; Lee, L.M.; Jenkins, H.; Britten, J.F.; Morim, D.R.; et al. Supramolecular Macrocycles Reversibly Assembled by Te ... O Chalcogen Bonding. *Nature Comm.* **2016**, *7*, 1–10. [CrossRef]
17. Ho, P.C.; Rafique, J.; Lee, J.; Lee, L.M.; Jenkins, H.A.; Britten, J.F.; Braga, A.L.; Vargas-Baca, I. Synthesis and Structural Characterisation of the Aggregates of Benzo-1,2-Chalcogenazole 2-Oxides. *Dalton Trans.* **2017**, *46*, 6570–6579. [CrossRef]
18. Werz, D.B.; Gleiter, R.; Rominger, F. Nanotube Formation Favored by Chalcogen−Chalcogen Interactions. *J. Am. Chem. Soc.* **2002**, *124*, 10638–10639. [CrossRef]
19. Gleiter, R.; Haberhauer, G.; Werz, D.B.; Rominger, F.; Bleiholder, C. From Noncovalent Chalcogen–Chalcogen Interactions to Supramolecular Aggregates: Experiments and Calculations. *Chem. Rev.* **2018**, *118*, 2010–2041. [CrossRef] [PubMed]
20. Huynh, H.-T.; Jeannin, O.; Fourmigué, M. Organic Selenocyanates as Strong and Directional Chalcogen Bond Donors for Crystal Engineering. *Chem. Commun.* **2017**, *53*, 8467–8469. [CrossRef] [PubMed]
21. Jeannin, O.; Huynh, H.-T.; Riel, A.M.S.; Fourmigué, M. Chalcogen Bonding Interactions in Organic Selenocyanates: From Cooperativity to Chelation. *New J. Chem.* **2018**, *42*, 10502–10509. [CrossRef]
22. Riel, A.M.S.; Huynh, H.-T.; Jeannin, O.; Berryman, O.; Fourmigué, M. Organic Selenocyanates as Halide Receptors: From Chelation to One-Dimensional Systems. *Cryst. Growth Des.* **2019**, *19*, 1418–1425. [CrossRef]
23. Huynh, H.-T.; Jeannin, O.; Aubert, E.; Espinosa, E.; Fourmigué, M. Chalcogen Bonding Interactions in Chelating, Chiral Bis(Selenocyanates). *New J. Chem.* **2021**, *45*, 76–84. [CrossRef]
24. Xu, Y.; Kumar, V.; Bradshaw, M.J.Z.; Bryce, D.L. Chalcogen-Bonded Cocrystals of Substituted Pyridine N-Oxides and Chalcogenodiazoles: An X-Ray Diffraction and Solid-State NMR Investigation. *Cryst. Growth Des.* **2020**, *20*, 7910–7920. [CrossRef]
25. Kumar, V.; Xu, Y.; Bryce, D.L. Double Chalcogen Bonds: Crystal Engineering Stratagems via Diffraction and Multinuclear Solid-State Magnetic Resonance Spectroscopy. *Chem. Eur. J.* **2020**, *26*, 3275–3286. [CrossRef]
26. Dhaka, A.; Jeannin, O.; Jeon, I.-R.; Aubert, E.; Espinosa, E.; Fourmigué, M. Activating Chalcogen Bonding (ChB) in Alkylseleno/Alkyltelluroacetylenes toward Chalcogen Bonding Directionality Control. *Angew. Chem. Int. Ed.* **2020**, *132*, 23789–23793. [CrossRef]
27. Dhaka, A.; Jeannin, O.; Aubert, E.; Espinosa, E.; Fourmigué, M. Supramolecular Rectangles through Directional Chalcogen Bonding. *Chem. Commun.* **2021**, *57*, 4560–4563. [CrossRef] [PubMed]
28. Capucci, D.; Balestri, D.; Mazzeo, P.P.; Pelagatti, P.; Rubini, K.; Bacchi, A. Liquid Nicotine Tamed in Solid Forms by Cocrystallization. *Cryst. Growth Des.* **2017**, *17*, 4958–4964. [CrossRef]
29. Aakeröy, C.B.; Wijethunga, T.K.; Haj, M.A.; Desper, J.; Moore, C. The Structural Landscape of Heteroaryl-2-Imidazoles: Competing Halogen- and Hydrogen-Bond Interactions. *CrystEngComm* **2014**, *16*, 7218. [CrossRef]
30. Zhang, Z.; Kim, D.S.; Lin, C.-Y.; Zhang, H.; Lammer, A.D.; Lynch, V.M.; Popov, I.; Miljanić, O.Š.; Anslyn, E.V.; Sessler, J.L. Expanded Porphyrin-Anion Supramolecular Assemblies: Environmentally Responsive Sensors for Organic Solvents and Anions. *J. Am. Chem. Soc.* **2015**, *137*, 7769–7774. [CrossRef] [PubMed]
31. Sheldrick, G.M. *Programs for the Refinement of Crystal Structures*; University of Göttingen: Göttingen, Germany, 1996.
32. Farrugia, L.J. WinGX and ORTEP for Windows: An update. *J. Appl. Cryst.* **2012**, *45*, 849–854. [CrossRef]
33. Frisch, M.J.; Trucks, G.W.; Schlegel, H.B.; Scuseria, G.E.; Robb, M.A.; Cheeseman, J.R.; Scalmani, G.; Barone, V.; Petersson, G.A.; Nakatsuji, H.; et al. *Gaussian 09, Rev. A.02*; Gaussian, Inc.: Wallingford, CT, USA, 2016.
34. Grimme, S.; Antony, J.; Ehrlich, S.; Krieg, H. A consistent and accurate ab initio parametrization of density functional dispersion correction (DFT-D) for the 94 elements H-Pu. *J. Chem. Phys.* **2010**, *132*, 154104. [CrossRef] [PubMed]
35. Keith, T.A. *AIMAll, Version 19.10.12*; TK Gristmill Software; Todd A. Keith: Overland Park, KS, USA, 2019. Available online: aim.tkgristmill.com (accessed on 13 December 2019).